0270-9139/89/0902-0285$02.00/0
HEPATOLOGY

Vol. 9, No. 2, pp. 285–296, 1989
Printed in U.S.A.

The Multiple-Indicator Dilution Technique for Characterization of Normal and Retrograde Flow in Once-Through Rat Liver Perfusions

MARIE V. ST-PIERRE, ANDREAS J. SCHWAB, CARL A. GORESKY, WAI-FONG LEE AND K. SANDY PANG

Faculty of Pharmacy and Department of Pharmacology, Faculty of Medicine, University of Toronto, Toronto, Ontario, and McGill University Medical Clinic, Montreal General Hospital, Montreal, Quebec, Canada

The technique of normal and retrograde rat liver perfusion has been widely used to probe zonal differences in drug-metabolizing activities. The validity of this approach mandates the same tissue spaces being accessed by substrates during both normal and retrograde perfusions. Using the multiple-indicator dilution technique, we presently examine the extent to which retrograde perfusion alters the spaces accessible to noneliminated references. A bolus dose of ^{51}Cr-labeled red blood cells, ^{125}I-albumin, ^{14}C-sucrose and $^{3}H_2O$ was injected into the portal (normal) or hepatic (retrograde) vein of rat livers perfused at 10 ml per min per liver. The outflow perfusate was serially collected over 220 sec to characterize the transit times and the distribution spaces of the labels. During retrograde perfusion, red blood cells, albumin and sucrose profiles peaked later and lower than during normal perfusion, whereas the water curves were similar. The transit times of red blood cells, albumin and sucrose were longer ($p < 0.005$), whereas those for water did not change. Consequently, retrograde flow resulted in significantly larger sinusoidal blood volumes (45%), albumin Disse space (42%) and sucrose Disse space (25%) than during normal flow, whereas the distribution spaces for total and intracellular water remained unaltered. The distension of the vascular tree was confirmed by electron microscopy, by which occasional isolated foci of widened intercellular recesses and spaces of Disse were observed. Cellular ultrastructure was otherwise unchanged, and there was no difference found between normal and retrograde perfusion for bile flow rates, AST release, perfusion pressure, oxygen consumption and metabolic removal of ethanol, a substrate with flow-limited distribution, which equilibrates rapidly with cell water (hepatic extraction ratios were virtually identical: normal vs. retrograde, 0.50 vs. 0.48 at 6 to 7.4 m*M* input concentration). These findings suggest that the functional and metabolic capacities of the liver remain unperturbed during retrograde perfusion, rendering the technique suitable for the investigation of zonal differences in drug-metabolizing enzymes.

The presence of uneven distribution of drug-metabolizing enzymes within the acinus of the intact liver has been studied by widely divergent techniques. Immunohistochemical and staining techniques (1–4) identify the presence and therefore the distribution of specific isoenzymes but seldom reveal the associated metabolic activities. This information may be provided by complementary, direct approaches that quantitate substrate disappearance/metabolite formation in discrete acinar regions by monitoring either changes in fluorescence or micro-reflectance (5–8), or from metabolic data derived from microdissection of tissues from various acinar regions (9). For these direct methods, the influence of coexisting pathway(s) and the mechanism(s) of substrate uptake mediated along the direction of flow are seldom considered. Selective zonal injury with quantification of residual enzymatic activity has shown variable success (10–12), since interpretation of metabolic data from this approach requires verification that such injury is confined to the intended region of the liver (12) and an assurance that flow patterns have not deviated from normal.

A quantitative description of substrate disappearance and metabolite formation within the intact liver requires consideration of microcirculatory events and the attendant heterogeneities of the organ, the most prominent being localization of enzymatic activities. As substrate flows from the inlet to the outlet of the liver, metabolic activity is progressively accrued, as successive hepatocytes are encountered along the sinusoid. Similarly, after a metabolite is generated within hepatocytes, the metabolite can potentially reenter the sinusoid and be subjected to successive actions of hepatocytes downstream in the direction of flow. An intact organ perfusion technique (13), with substrate delivery in the forward (anterograde or normal, N) and reverse directions (retrograde, R) to perfused livers, has been used to probe heterogeneous distributions of metabolic activities of multienzyme systems (14, 15). By reversing the flow direction and main-

Received February 19, 1986; accepted July 22, 1988.
This work was supported by the Medical Research Council of Canada, the Canadian Liver Foundation, the National Institutes of Health (GM-38250), the Quebec Heart Foundation and the Fast Foundation.
This work was presented in part at the Annual Meeting of the American Association for the Study of Liver Diseases, Chicago, 1987, and was published in part as an abstract (Hepatology 1987; 7:1129).
Address reprint requests to: K. S. Pang, Ph. D., Faculty of Pharmacy, University of Toronto, 19 Russell St., Toronto, Ontario, Canada M5S 2S2.

taining an invariant inlet concentration within the same liver preparation, the substrate enters the liver from the hepatic vein. Inasmuch as the recruitment of enzymatic activity is mediated along the direction of flow, R perfusion effectively reverses the order of recruitment of drug-metabolizing activities. Normal and retrograde (NR) perfusion compares the relative distribution of at least two enzymatic systems. It will not discern the distribution patterns of uni-enzyme systems (*i.e.* where substrate is metabolized to form only one metabolite), but it will delineate zonal enrichment of enzymes for metabolite formation and metabolism in sequential pathways. The hepatic extraction ratio of drug (E) remains constant, whereas the extent of sequential metabolism of the primary metabolite, reflected by efflux of primary and secondary metabolites, will differ (14, 15). The NR technique also readily delineates relative enzymatic distributions of competing pathways when metabolites do not endure further metabolism. This is exemplified by sulfation and glucuronidation of phenolic substrates (16, 17). At low inlet substrate concentration ($C_{In} \ll K_m$, for all pathways), the ratios of metabolite formation rates differ; at intermediate C_{In} ($<K_m$ of glucuronidation but $>K_m$ of sulfation), both E and the ratio of metabolite formation rates differ. While the rate-determining step of the metabolic reaction (*e.g.* cosubstrate supply, enzyme activity or presence of a diffusional barrier) is not identified, the overall reaction rate and enzymatic parameters, K_m and V_{max}, sometimes involving multiplicity of isozymes with overlapping specificities, are assessed.

NR perfusion of the rat liver has been used to probe zonal metabolic (6, 7, 14, 16, 18, 19), excretory (20), transport (21) or biosynthetic (22, 23) functions. Comparison of metabolic/disposition data derived from N and R perfused livers ordinarily assumes an equal access by the substrate to all hepatocytes. Although no impairment in the functional integrity of the organ has been reported, distension of the sinusoids and the space of Disse was noted during electron microscopy of R perfused livers (24). This emphasized the need for a systematic and quantitative investigation into the changes induced by R perfusion. The multiple-indicator dilution technique (25) was employed to characterize the behavior of noneliminated vascular (^{51}Cr-RBC), extracellular (^{125}I-albumin, ^{14}C-sucrose) and intracellular (^{3}H-water) references in N or R perfused rat livers. Transit times and distribution volumes for these labels were compared after N and R flows. Changes in these parameters should reflect significant alterations at the microcirculatory level.

Metabolic capacity of the perfused organ was assessed by determining the extraction of ethanol after N and R delivery. Since ethanol resembles water in its flow-limited uptake into parenchymal cells and its distribution space (26), an identical recruitment of hepatocytes will be reflected by the same E values during both N and R flow. By properly choosing the inlet concentration (6 to 7 m*M*) to result in an intermediate E (0.5), substrate supply will not be rate limiting for recruitment of alcohol dehydrogenase (27), an evenly distributed enzyme system (28). At low ethanol concentrations, E is almost complete and uptake will be carried out predominantly by upstream hepatocytes (periportal during N perfusion and perihepatic venous during R perfusion), failing to test ethanol metabolic function in all zones of the liver; at high-input ethanol levels, changes in E will be imperceptible. Adjunctive viability tests, electron microscopy, biochemical (AST, glucose, potassium, oxygen consumption), bile flow and perfusion pressure measurements, were also performed.

MATERIALS AND METHODS

Liver Perfusion. Male Sprague-Dawley rats (Charles River Canada, Inc., St. Constant, Quebec, Canada) (320 to 375 gm) were used as liver (9 to 14 gm) donors. Animals were anesthetized intraperitoneally with sodium pentobarbital (50 mg per kg), and the livers were perfused in a once-through (nonrecirculating) system as previously described (14). Briefly, the bile duct was cannulated (PE-20), and an intravenous placement catheter unit (14-gauge, 2 inches; Deseret Medical Inc., Sandy, UT) was inserted into the portal vein. Perfusion was begun immediately. An identical catheter was introduced into the thoracic inferior vena cava (hepatic vein), from which effluent perfusate was sampled during N perfusion experiments. R perfusion experiments required switching the inflow from the portal to the hepatic venous cannula, allowing collection of the effluent from the portal vein. Perfusate composition was identical to that previously described (14) and was delivered at 10 ml per min per liver. The influent perfusate was saturated with a flow of 95% O_2 and 5% CO_2 (1 liter per min). Bile flow (μl per min per gm liver) was monitored throughout N or R perfusions (60 min) and averaged over 10-min intervals. The inflowing perfusion pressure was monitored by means of an open vertical tube in the segment between the pump and the liver.

Multiple-Indicator Dilution. Multiple-indicator dilution experiments were performed in livers after a 30- to 35-min stabilization period. Each liver preparation was subjected to a single flow direction. The injection bolus (0.1 ml), prepared according to Goresky (25), contained ^{51}Cr-labeled RBC (0.15 μCi), ^{125}I-labeled albumin (2.2 μCi), ^{3}H-labeled water (13 μCi) and ^{14}C-labeled sucrose (1.3 μCi), but was otherwise identical in composition to the perfusate. The injection site was similar to that described in another report (29). Prior to tracer injection, perfusate flowed freely through a bifurcation. Seconds before tracer administration, the injection side arm was clamped distal to the injection port, and the dose was slowly introduced. The simultaneous release of this clamp of the injection arm and clamping of the alternate arm diverted the inflowing stream through the injection side at the requisite flow rate. A fraction collector was activated. The venous outflow was serially collected from the portal (R) or hepatic (N) outflows at successive intervals of 1 sec, progressively lengthening to 2 and then 4 sec for a total of 220 sec. The volume of injected material was determined gravimetrically, by dividing the weight of the injected material by the density of the fluid (1.05). The hematocrit was determined in outflow samples (Model M.B., International Equipment Co., Needham Heights, MA). The ^{51}Cr and ^{125}I radiolabels in blood aliquots (30 to 200 μl) were quantified (Model 5500 gamma counter, Beckman Instruments, Inc., Palo Alto, CA), after correction for the spillover of ^{51}Cr activity (channel 2) into the ^{125}I photopeak. After centrifugation, the remaining plasma was diluted (1:4 v/v) with acetonitrile to precipitate the albumin. ^{3}H and ^{14}C activities in the supernatant were quantified by liquid scintillation counting (Beckman LS-6800 counter) after quench correction by an external standard method. Radioactivity meas-

urements for each tracer were expressed as a fraction of the injected dose per ml (units of fraction of dose per ml).

The concentrations of RBC, albumin and sucrose labels were less than 0.1% of peak values at the end of the collection interval (220 sec). Semilogarithmic plots of the normalized data vs. time revealed a late linear downslope for the water curve and allowed estimation of a terminal rate constant, k (2.303 × (−)slope). The area under the curve (AUC $|_0^t$) and area under the time-activity product vs. time curve (AUMC $|_0^t$) up to the last sampling point, t, were calculated by the trapezoidal rule. The total AUC and AUMC (from t = 0 to t = ∞) were estimated by the sum of the sampled area and the area under the curve extrapolated beyond the last collected sample (29):

$$AUC = AUC|_0^t + \frac{C_{last}}{k} \quad (1)$$

$$AUMC = AUMC|_0^t + C_{last}\left(\frac{t_{last}}{k} + \frac{1}{k^2}\right) \quad (2)$$

where C_{last} and t_{last} are the concentration (fraction of dose/ml) and time for the end interval of the last sampling point for ^3H_2O.

The mean transit times ($\bar{t}$) of the labels in the system were calculated by moment analysis as (30):

$$(\bar{t}) = \frac{AUMC}{AUC} \quad (3)$$

The transit times through the injection device and collection catheter ($\bar{t}_{cath}$, 6.5 sec) were determined from the volume of blood filling the tubings and catheters from the point of injection to the tip of outflow and the flow rate; this was subtracted from the transit times of the markers ($\bar{t}$) to provide estimates of the transit times of the labels through the liver, $\bar{t}$.

The distribution space for each label, V, was determined as the product of the transit times ($\bar{t}$) and the appropriate flow rates, Q:

$$V = Q \times (\bar{t}) \quad (4)$$

Sinusoidal blood volume, albumin and sucrose distribution spaces and water spaces were estimated by use of the respective blood (Q_B), plasma (Q_P), and water flows (Q_W), after correcting for hematocrit (Hct), and the water contents of red cell (f_{RBC} = 0.7 ml per ml) and plasma (f_P = 0.98 ml per ml when 1% albumin is present):

$$Q_P = Q_B(1 - Hct) \quad (5)$$

$$Q_W = Q_B\ Hct\ f_{RBC} + Q_B f_P(1 - Hct) \quad (6)$$

Cellular water space was calculated as the difference between total and the sum of plasma and red blood cell water spaces.

Metabolism. Ethanol metabolism studies were comprised of three 40-min perfusion periods; initial (N or R) flow, reverse perfusion (R or N, respectively) and a return to initial conditions, a procedure routine in metabolism studies to ensure that the extraction efficiency of the organ has remained constant throughout the experiment. Ethanol (6 to 7.4 m*M*) was delivered (10 ml per min per liver) once-through the rat liver preparation. The effluent was sampled under steady-state conditions when the rate of substrate efflux into perfusate was constant.

Ethanol in input and output blood perfusate samples was quantified by headspace gas-liquid chromatography (31). Calibration curves were prepared by spiking blank perfusate (0.3 ml) with aliquots (10 to 50 μl) of ethanol standards (20, 200, 1,250 μl per 100 ml glass-distilled water) and 25 μl of aqueous *n*-propanol (Burdick Jackson, Muskegon, MI) as the internal standard. The ratio of the areas of ethanol to internal standard vs. spiked concentrations of ethanol was plotted and regressed to provide a slope and an intercept. All collections and transfers of sample were effected over ice. After addition of the internal standard, samples (0.3 ml) were vortexed and incubated at 60°C in a rotating water bath for 20 min. A Pressure-Lok gas tight syringe (Precision Sampling Corp., Baton Rouge, LA) retrieved 1.0 ml of the ethanol vapor. The vapor was compressed to 0.2 ml volume and injected into a gas-liquid chromatograph (HP 5880A, Hewlett Packard, Palo Alto, CA) equipped with a flame ionization detector. Separation was achieved by a 5% Carbowax 20M on 80/120 Carbopack B column (Supelco, Mississauga, Ontario, Canada). The chromatography conditions were: oven temperature: 70°C; injector temperature: 150°C; detector temperature: 200°C; air flow: 300 to 400 ml per min; nitrogen: 28 to 38 ml per min; hydrogen: 28 to 30 ml per min. The retention times were: ethanol: 2.06 min; *n*-propanol: 4.70 min; run time: 6 min. Acetaldehyde eluted prior to ethanol and did not interfere in the assay. The sensitivity limit of the assay was 0.015 m*M*, and the coefficients of variation at 16.5, 1.65 and 0.015 m*M* were <6.6%.

Microscopy. Livers undergoing microscopic assessment were randomly assigned to four experimental groups: (a) control (perfusion fixation only); (b) 60 min N perfusion (perfusion with drug-free medium followed by perfusion fixation); (c) 60 min R perfusion (R perfusion with drug-free medium followed by perfusion fixation), and (d) normal:retrograde:normal (NRN) perfusion (three 40-min periods followed by perfusion fixation). The optimal *in situ* fixation procedure was a modification of existing methods (32, 33): ice-cold 0.9% sodium chloride (approximately 10 ml) was infused through the portal vein, followed by perfusion at 10 ml per min per liver of fixative medium (4% formaldehyde, 1% glutaraldehyde in 200 m*M* phosphate buffer) for 10 min. Small tissue slices were excised from the left, right main and caudate lobes and immersed in fixative for 1 hr. Specimens were postfixed in 1% osmium tetroxide/1.5% potassium ferricyanide solution for 30 min, dehydrated in acetone and embedded in Epon/Araldite. Thick sections (0.5 to 1 μm) were stained with toluidine blue and examined by light microscopy. Selected tissue blocks (containing both a terminal portal venule and a terminal hepatic venule) were thin sectioned and viewed under a Philips 300 electron microscope.

Biochemistry. Baseline control values of the perfusate were determined prior to perfusion. At 30-min intervals during each perfusion period, effluent was collected for AST, potassium and glucose determinations. AST levels were measured by ultraviolet spectrophotometry at 340 nm using Sigma-Kit premixed reagents (Sigma Technical Bulletin No. 55-uV, Sigma Diagnostics, St. Louis, MO). Potassium concentrations were measured by flame photometry (IL 943, Instrumentation Laboratory, S.P.A., Milan, Italy). Glucose was measured by means of a Beckman Glucose Analyzer 2 (Beckman Instruments, Inc., Brea, CA). The oxygen content in inflow and outflow perfusate was measured using a Clark-style oxygen electrode (Instech Laboratories, Inc., Horsham, PA) and calculated (μmoles per min per gm liver) using the relationship (34):

$$O_2\ content = \alpha * PO_2 + 1.39 * (Hb) * \%\ saturation/100 \quad (7)$$

where α is the solubility of oxygen in blood at 37°C. The rate of oxygen consumption was calculated from the inflow-outflow concentration difference times the blood flow. Hemoglobin concentration (gm per 100 ml) (Hb), was measured using the cyanomethemoglobin method (35).

Statistical Analysis. Differences between the N and R treatment of perfused livers were assessed by the unpaired

Student's t test. The criterion for statistical significance was $p < 0.05$.

RESULTS

Multiple-Indicator Outflow Dilution Curves. Representative sets of outflow dilution curves are presented (Fig. 1). The initial delay in appearance of label reflects the catheter, large vessel and shortest sinusoid transit times. During both modes of perfusion, the RBC profiles peaked earliest and highest, decayed the fastest and were associated with the shortest $\bar{t}$ (Table 1). The peaks of albumin and sucrose, substances with access to

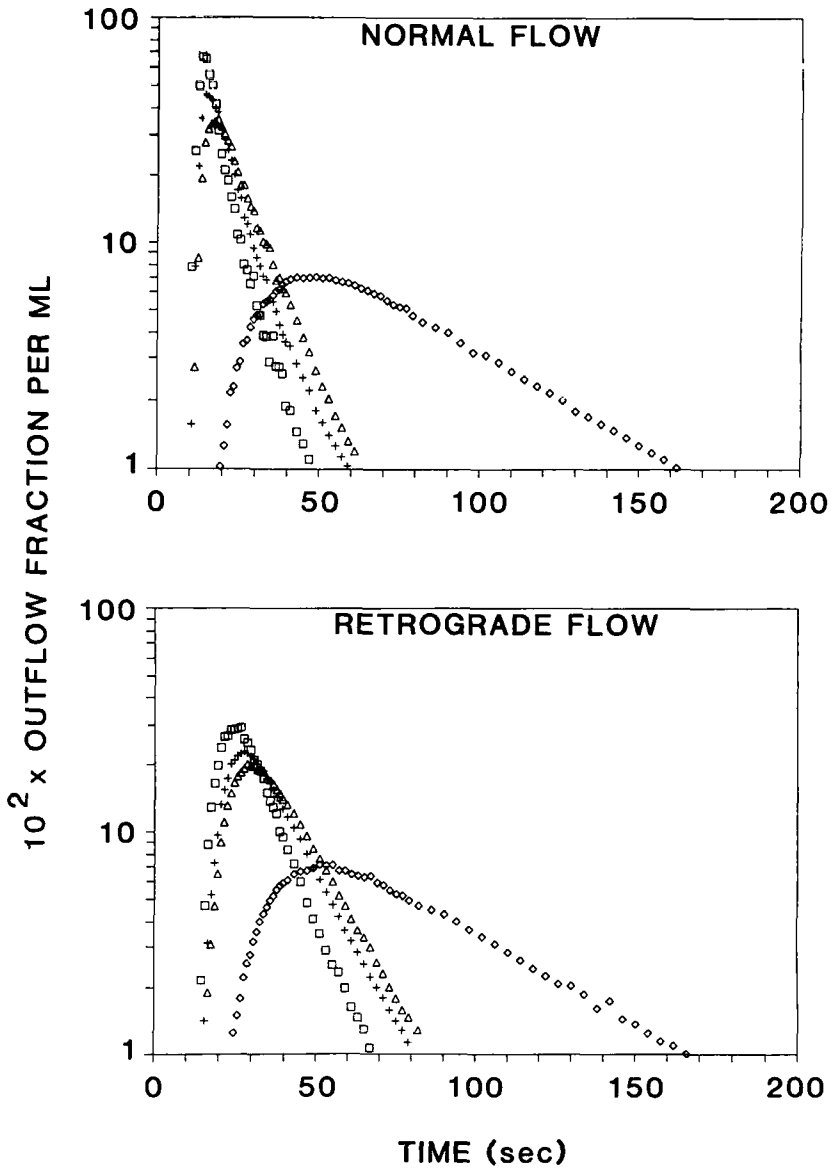

FIG. 1. Representative hepatic outflow indicator dilution curves from once-through normal and retrograde rat liver perfusions (10 ml per min per liver). Livers were perfused with blood perfusate for 30 min prior to a bolus injection of the noneliminated radiolabeled references, ^{51}Cr-labeled RBC (□), ^{125}I-labeled albumin (+), ^{14}C-sucrose (△) and ^{3}H-water (◇) into the portal (N) or hepatic (R) veins. Values for the *y* axis are outflow concentrations which have been normalized for the injected dose, and values on the *x* axis represent time elapsed after the injected dose. The time is uncorrected for catheter and large vessel transit times.

TABLE 1. **Transit times and distribution spaces through normal and retrograde perfused livers (n = 6)**

Flow direction	Liver weight (gm)	Flow rate (ml/min/gm liver)	Transit times (sec)[a]				Distribution spaces (ml/gm liver)						
			RBC	Albumin	Sucrose	Water	Sinusoidal blood volume	Total albumin space	Total sucrose space	Albumin Disse space	Sucrose Disse space	Total water space	Cellular water space
Normal													
Mean	11.3	0.91	15.23	18.82	21.56	71.20	0.20	0.24	0.28	0.045	0.08	0.99	0.69
S.D.	1.7	0.15	2.59	2.35	2.31	8.30	0.06	0.06	0.06	0.008	0.01	0.09	0.05
Retrograde													
Mean	11.82	0.86	22.93[b]	28.32[b]	31.23[b]	77.12	0.29[b]	0.34[b]	0.37[b]	0.064[b]	0.10[b]	1.02	0.62
S.D.	1.39	0.10	4.17	4.17	4.97	10.34	0.05	0.06	0.07	0.004	0.01	0.10	0.08

[a] Transit times are corrected for inflow and outflow catheter delays.
[b] Statistically significant, $p < 0.005$, for normal vs. retrograde flow.

the Disse space, were progressively delayed and depressed relative to that of the RBC. The displacement time and depression of the peak concentrations were most marked for labeled water, which enters the intracellular water space.

The shapes of the curves for the vascular and extracellular markers (RBC, albumin, sucrose) were different during N and R perfusion (Fig. 1). The profiles rose more sharply and the declines were steeper after N perfusion. Contrastingly, labeled red blood cells, albumin and sucrose emerged later during R perfusion; RBC, albumin and sucrose exhibited an approximate 50% increase in $\bar{t}$ when compared to N perfusion (Table 1). The labeled water outflow pattern was indistinguishable in R and N perfused livers, and $\bar{t}$ for ^3H_2O in N and R perfusions was not statistically different. Superimposition of the diffusible label profiles onto the RBC curve was carried out as described previously (25) (Fig. 2). The fitting and superimposition procedures provided estimates of large vessel values (t_o) (N vs. R, 2.04 ± 1.4 and 2.82 ± 1.8 sec) and large vessel volumes (N vs. R, 0.03 ± 0.02 and 0.04 ± 0.02 ml per gm liver), which did not differ significantly during N and R perfusion. The effective superimposition indicates that each diffusible label is distributed in a delayed wave flow-limited fashion within the liver (25). The mean sinusoidal volume, found after appropriate subtraction of the volume of the large vessel from the total red blood cell volume, was significantly enlarged during R perfusion, as was the albumin Disse space (Table 1). The Disse space accessible to sucrose was also enlarged volumetrically during R perfusion, to the same extent, whereas change in the total water space was not statistically identifiable. After subtraction of the intravascular and extracellular water spaces, the intracellular water volume was also found not to differ significantly (N vs. R, 0.69 ± 0.05 vs. 0.62 ± 0.08 ml per gm liver) (Table 1). The behavior of the noneliminated markers during R perfusion was similar to that observed in rat livers perfused at higher flow rates (29).

Metabolism. Ethanol metabolism did not change as

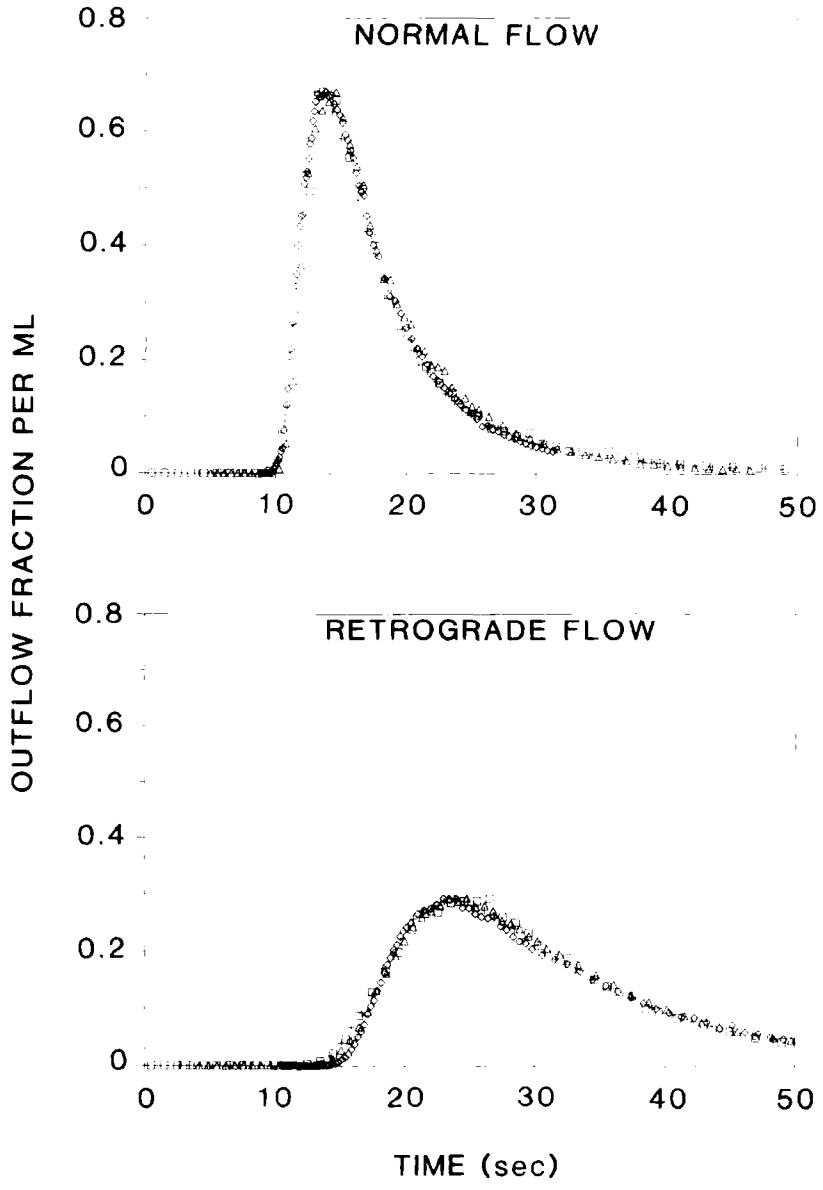

FIG. 2. Representative hepatic outflow indicator dilution curves after adjusting concentration and time values by the factor $(1 + \gamma_{AD})$, $(1 + \gamma_{SD})$ and $(1 + \gamma_W)$ and $[1/(1 + \gamma_{AD})]$, $[1/(1 + \gamma_{SD})]$ and $[1/(1 + \gamma_W)]$, respectively (γ_{AD} is the ratio of albumin Disse space to plasma space, γ_{SD} is the ratio of sucrose Disse space to plasma space and γ_W is the ratio of the sum of intracellular water and Disse water space to sinusoidal water space). Superimposition of the adjusted diffusible labels (albumin, sucrose and water, same symbols as Fig. 1) on the labeled RBC curve is apparent for both N and R data sets.

a function of direction of substrate delivery in this NRN design. The mean hepatic extraction ratio (E), after N (0.50 ± 0.11) and R perfusions (0.48 ± 0.10) was not different. The preparations remained stable despite the perturbations of flow and regardless of the order of perfusion (NRN or RNR) (Fig. 3). Biliary excretion accounted for less than 0.15% of the dose.

Microscopy. The perfusion rate for fixative avoided excessive inflow pressure and did not damage the sinusoidal endothelium (32, 33). Preperfusion of the livers with saline rendered the sinusoids almost devoid of residual red blood cells. Figure 4a illustrates a micrograph of a midzonal hepatocyte from a control preparation. The sinusoids are patent with intact fenestrated endothelium. Numerous microvilli within intercellular recesses and on the sinusoidal faces of the hepatocytes protrude through the space of Disse to appose the surface of the endothelial cells. Electron micrographs of the 60-min N perfusion (Fig. 4b) and R perfusion (Fig. 4c) were comparable to control livers. The space of Disse is closely apposed to the endothelial lining. Mitochondria are numerous, with membranes, cristae and matrix granules intact.

After successive N and R perfusions (Fig. 4d), the preparations were qualitatively similar. However, isolated foci of enlarged intercellular recesses and spaces of Disse were found. Microvilli tended to be less numerous in these areas. Both zone 1 and zone 3 cells were equally affected, but parenchymal cells were otherwise normal. Glycogen stores were observed and mitochondrial changes were absent.

Biochemical and Physical Measurements. Perfusate levels of potassium were not elevated above mean control values (K^+ = 5.6 ± 0.2 mEq per liter) for the 60-min N perfused experiments nor did the levels increase above the control value during the 60-min R or NRN experiments. A transient increase in glucose levels occurred. This 20% elevation over baseline values (300 mg%) was followed by a gradual decline (data not shown). Perfusion for 60 min in either direction was associated with a minimal increase in effluent plasma AST above baseline levels (Fig. 5). The concentrations of AST were lower for R experiments (Fig. 5a). During perfusion in the NRN sequence, outflow plasma levels of AST increased from baseline levels of 5.2 ± 1.4 units per liter to a peak of 9.1 ± 1.4 units per liter in the third period, but stayed within the defined limits of normalcy for the liver.

Mean values for bile flow rates, determined at 10-min intervals, are plotted vs. the midpoint of the collection interval (Fig. 6a). Bile flow in the R group was less during the first 10-min interval ($p < 0.05$). Subsequent collections showed no difference, regardless of the direction of perfusion. The rate of O_2 consumption was recorded at 5-min intervals, immediately following the multiple indicator dilution studies, in N or R perfused livers (Fig. 6b). When averaged over time (30 min), the rate of O_2 uptake was not different in N vs. R experiments (2.57 ± 0.40 vs. 2.37 ± 0.25 μmoles per min per gm liver, respectively). O_2 consumption did not change appreciably over the course of the experiment and approximated the reported basal *in vivo* level of 2.2 μmoles per min per gm liver (36–39). Inflow venous pressure averaged 8.64 ± 2.08 cm H_2O during NRN and 9.70 ± 1.33 cm H_2O during RNR perfusion. Values were not dependent on flow sequence nor direction of perfusion and remained stable throughout the experiment.

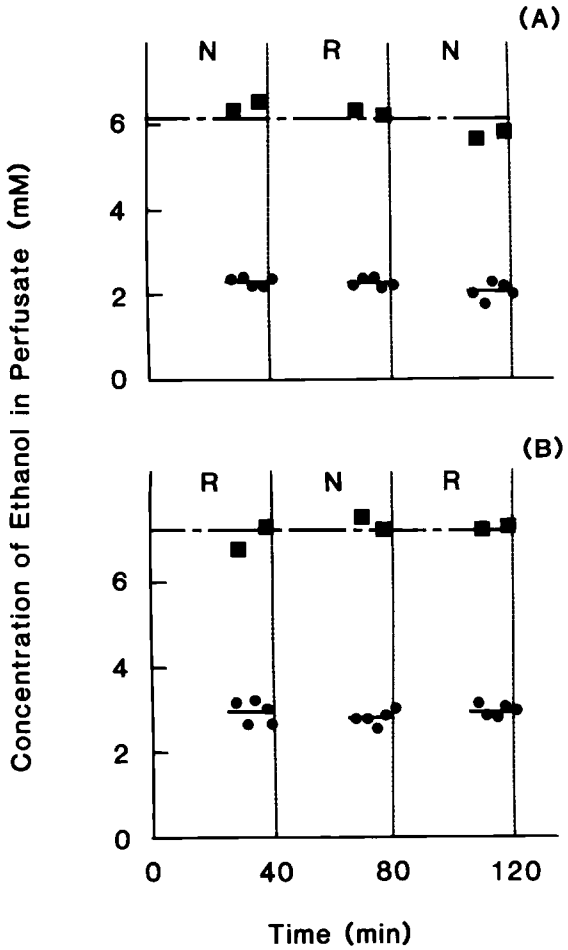

FIG. 3. Lack of change in ethanol metabolism during normal (N) and retrograde (R) flow to the same rat liver at constant perfusate flow of 10 ml per min per liver. In study (A), normal perfusion was followed by retrograde perfusion, after which initial conditions were resumed. In study (B), the order of perfusion was reversed. ■ and ● = the influent and effluent ethanol concentrations, respectively; —— - —— and —— = the corresponding averaged values.

DISCUSSION

Our viability tests failed to suggest loss of liver function during R perfusion. Although an appearance of enzymes in the effluent would normally indicate disruption of cell membranes, the minor increase in AST over baseline levels may be attributed to a time-dependent hemolysis of the RBCs (40, 41) induced by the rotating cylinder oxygenator, elevating even reservoir perfusate AST concentrations over a period of 1 to 3 hr. The initial increase of glucose above control levels is commonly observed in perfused livers of fed rats, and release of epinephrine secondary to denervation of the organ and decrease in portal pressure have been listed as possible causes (41, 42). Bile flow was not altered in the N and R

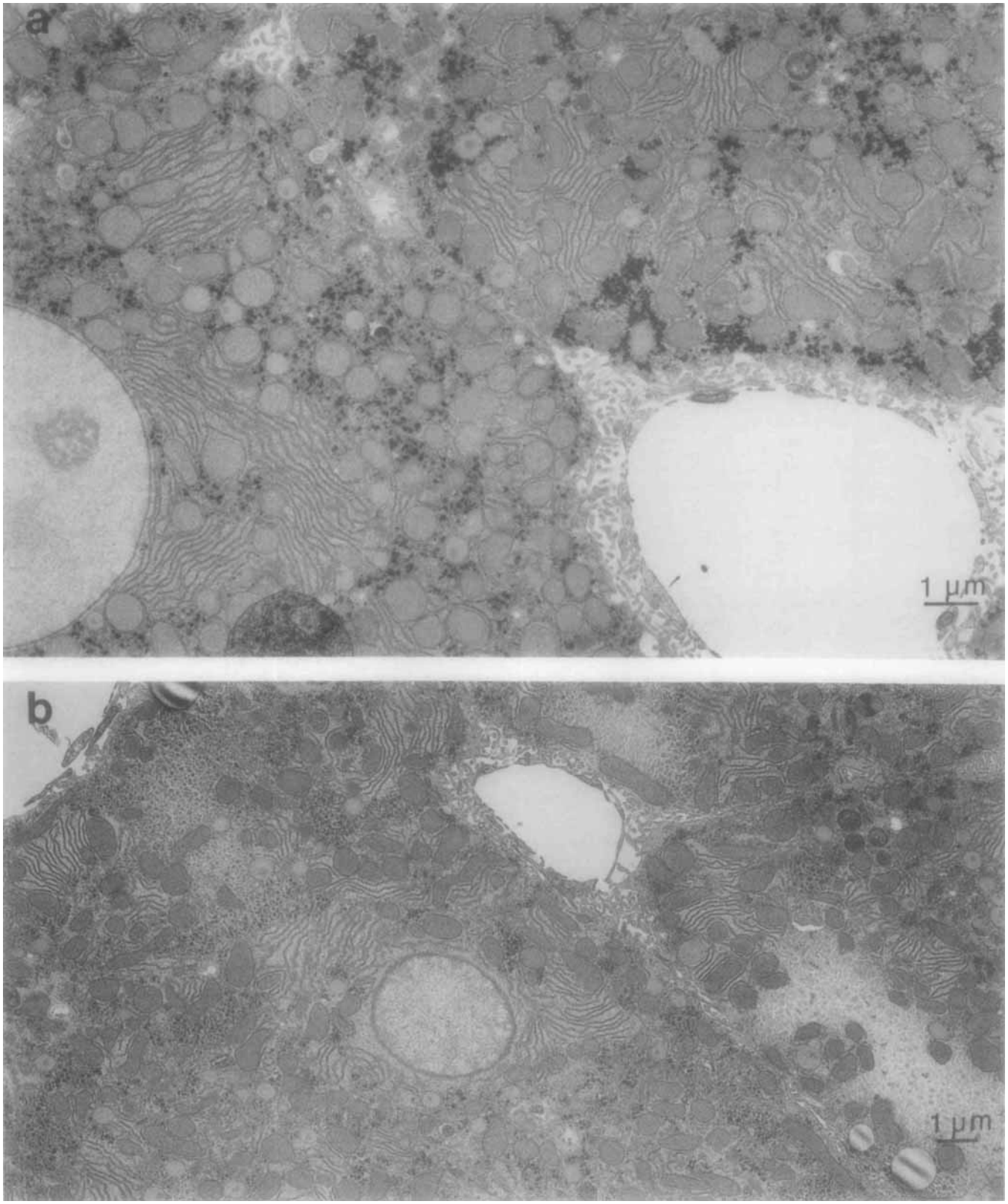

FIG. 4 (a and b). Transmission electron microscopic view of hepatocytes from perfused rat livers. Sections were stained with uranyl acetate and lead citrate. (a) Midzonal hepatocyte from control preparation demonstrating normal ultrastructure. × 9,600. (b) Zone 3 hepatocyte from rat liver perfused normally for 1 hr. The fenestrated endothelial lining is intact and numerous microvilli are present. × 7,200. (c) Zone 3 from rat liver perfused for 1 hr in the retrograde direction. The sinusoidal face of the hepatocyte is apposed to the endothelial lining. Numerous microvilli are present. A fat-storing cell lies within the space of Disse. × 7,400. (d) Zone 3 cell from liver perfused for a total of 120 min in a normal:retrograde:normal sequence. Fenestrated endothelial lining is intact. Normal ultrastructural morphology is observed. × 6,500.

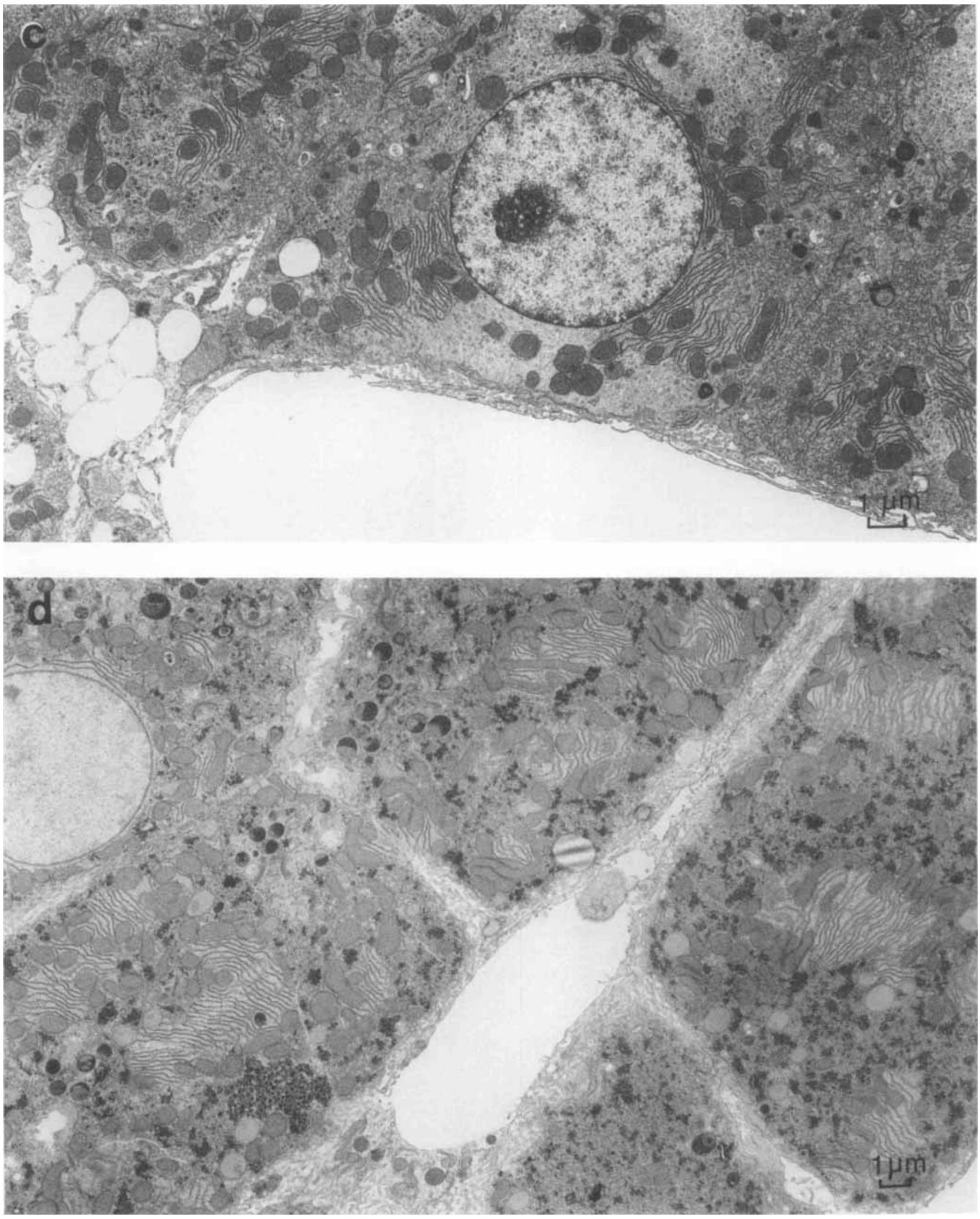

FIG. 4 (c and d).

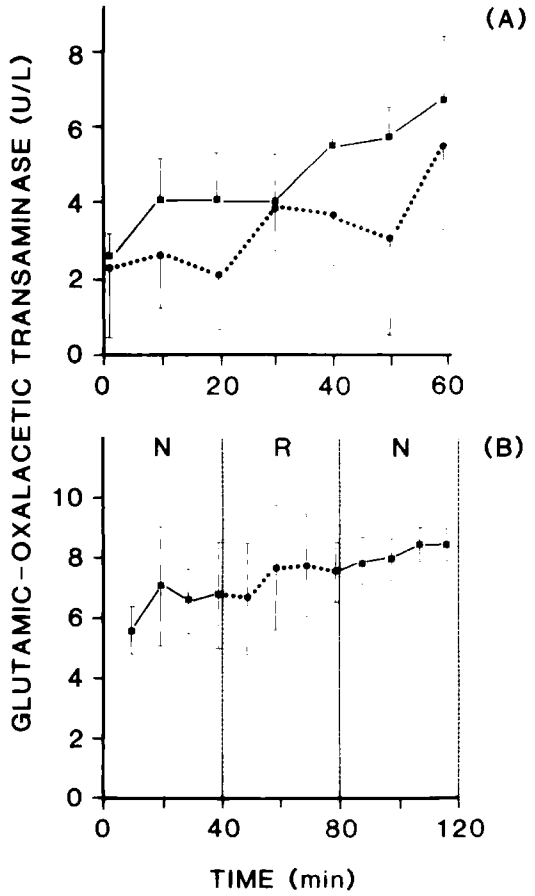

. 5. Time course of AST release into effluent after normal or ograde perfusion of the single-pass rat liver preparation. (A) Livers were perfused for 1 hr and outflow perfusate during normal (■) or retrograde (●) perfusions was collected every 10 min for AST determinations. For these experiments (n = 4 for N or R), the AST activity was consistently lower during retrograde flows. (B) Livers were perfused for three 40-min periods: normal:retrograde:normal. AST during N (■) and R (●) were determined at 10-min intervals. The maximum AST activity was 9 units per liter.

preparations (Fig. 6a), which is a consistent finding among investigators (14, 18, 21 24). Oxygen uptake by the whole organ during both N and R perfusion was unaltered (Fig. 6b). N and R perfusions with cell-free medium have also resulted in constant oxygen consumption across the perfused liver (18, 21, 24, 43). The lack of significant changes in the biochemical parameters is consistent with all previous reports (18, 21, 24).

Our microscopic findings indicate that normal ultrastructure is maintained in N and R perfused livers. However, in livers subjected exclusively to R flow or to alternating periods of N and R flows (NRN), there are scattered occurrences of enlarged sinusoids and widened spaces of Disse. These changes were more frequent in NRN perfused organs, perhaps attributable to the physical consequence of the two precipitous changes of flow. Investigators using a red blood cell-free perfusate at higher flow rates have similarly reported ultrastructural data consistent with distension of zone 3 sinusoids (18, 24), with morphometric analysis showing that sinusoids comprised a larger proportion of total tissue area after R perfusion (24). Given the constant perfusion pressure observed during R perfusion, and the constant transhepatic pressure previously reported using R flow at 2 ml per min per gm liver (21), it appears that zone 3 sinusoids may have distended to accommodate the higher pressure that occurs at the hepatic inlet, whereas total intrahepatic resistance remains unchanged.

A quantitative expression of these findings is provided by estimates of vascular and extravascular label transit times and their associated volumes of distribution. R perfusion induced a large increase in sinusoidal blood volume (45%), total albumin space (41%), albumin Disse space (42%), total sucrose volume (32%) and sucrose Disse space (25%) when compared to N perfusion (Table 1). The volumetric increases in sucrose space were, however, of the same order as those observed with albumin. Sucrose Disse space (representing 29 and 27% of total sucrose space for N and R, respectively) occupies virtually all the available Disse space, whereas albumin Disse space (representing 19% of the total albumin space for N and R perfusion), as a result of a polymer-excluded volume effect, ordinarily occupies about 60% of the total Disse space. Whereas the enlargement in the sucrose and albumin Disse spaces reflects a real distension of the Disse space, that for albumin also reflects an increase in the fraction of the total Disse space accessible to albumin, from 56 to 64%. The increase occurs because, even though the space is distended, the number of fixed polymer molecules in the space and their volumetric exclusion effects will not have changed.

The distensibility of the extracellular space is substantial. An increase (>100%) in total sucrose volume has, for instance, also been reported for R perfusion in single-indicator (sucrose) dilution studies performed with a plasma flow of 2 ml per min per gm liver (21); and a progressive increase in the distribution spaces for labeled red blood cells, albumin and sucrose was noted in rat livers perfused at increasing flow rates (8 to 16 ml per min) with the multiple-indicator dilution method (29). These mirror the kind of change encountered across a wide range of flows in the intact dog liver *in vivo* (44).

Although a significant increase in vascular and Disse space volumes was observed during R perfusion, this was not accompanied by an expected corresponding significant increase in total water space. It appears that our inability to perceive this lies in the relative magnitudes of the spaces being measured and their degree of variation. The standard deviation of the measurement for the water space was, in absolute terms, an order of magnitude larger than that of the vascular and interstitial spaces; it was in fact, larger than the absolute magnitudes of those spaces.

When the concentrations and times of the albumin, sucrose and water outflow profiles were appropriately adjusted (25), all curves became superimposable (Fig. 2). Both families of curves (N and R) performed equally well. A general interpretation of this observation is that N or R perfusions have not compromised hepatic architecture to a degree that would alter flow-limited distribution of diffusible labels within the liver.

The metabolic data on ethanol extraction are highly correlated with the findings from multiple-indicator di-

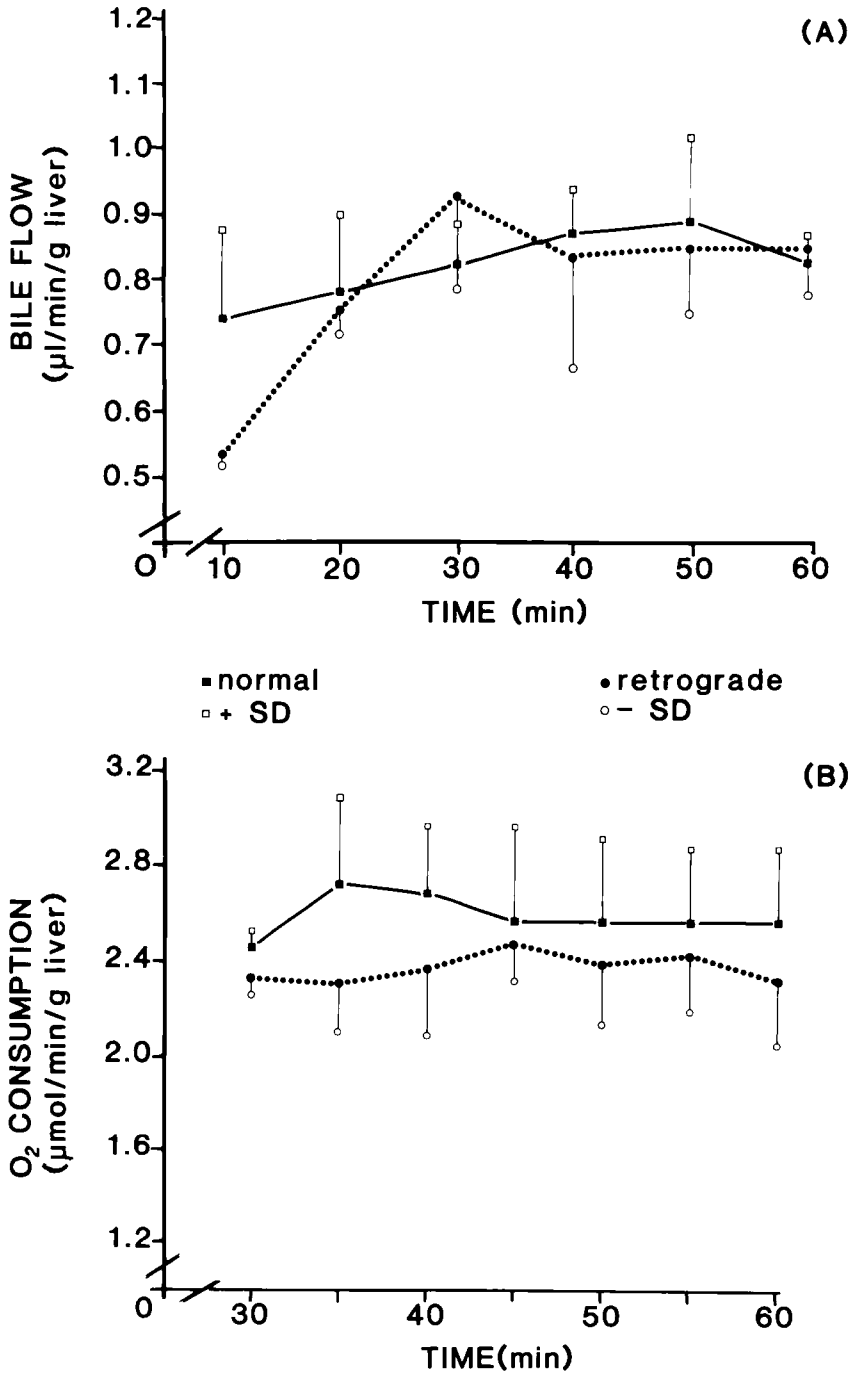

FIG. 6. Bile flow and oxygen consumption of N and R single-pass perfused rat livers. (A) Bile flow rate was not different when values for N (n = 5) or R (n = 5) were compared at time points beyond the initial 10-min interval. (B) Oxygen consumption during N and R was continuously monitored, and the mean values (n = 5) are plotted at 5-min intervals. Consumption of oxygen was not statistically different for N and R.

lution studies; both the intracellular water space (Table 1) and ethanol extraction capacity (Fig. 3) during N and R perfusion remained unaltered. An identical recruitment of activities by N or R flow has also been observed for acetaminophen, which, at tracer inlet concentration to the perfused rat liver, is converted solely to the sulfate conjugate predominantly by periportal hepatocytes (14, 45, 46). An unchanged metabolic recruitment of hepatocyte activities by each of these substrates appears to have occurred and suggests that the same hepatocytes are accessible during both N and R perfusions, regardless of metabolic zonation patterns.

It may be argued that a reversal of oxygen gradient (43) during R perfusion might alter rates of metabolic reactions. Whereas the zonal predominance of glycolysis and gluconeogenesis (47, 48) have been observed to shift with R perfusion, a similar reversal in the zonation of drug-metabolizing activities has not been observed. For substrates which are metabolized by parallel, competing pathways, however, decreases or increases in E during R when compared to N perfusion, have been observed (16, 18, 19, 49). The metabolic changes may be fully explained on the basis of regional enzyme enrichment and the kinetic constants for the pathways (16, 17, 19, 49) and not by a reversal of the acinar oxygen gradient.

Although the NR perfused liver is presently characterized by the multiple-indicator dilution technique in our system, the observations are expected to differ for other

experimental conditions with different perfusate compositions and flow rates. Especially for cell-free perfusions, where higher perfusate flow rates are required to maintain adequate oxygenation, the distribution characteristics of labeled references and viability parameters may change. Since all our present data provided validation that intracellular water space is conserved during retrograde perfusion, application of the procedure for probing the phenomenon of uneven distribution of drug-metabolizing activities in liver appears reasonable. The approach of comparing N and R perfusion will be particularly useful in the analysis of the underlying stacking of enzymes (their respective localizations in space), when successive drug and metabolite processing is being considered. This application of examination of zonation of enzymes in sequential metabolic pathways has been used, for example, to investigate phenacetin *O*-deethylation to form acetaminophen, with subsequent sulfation of acetaminophen. If the enzymes were stacked in space in such a fashion that, in relation to the ordinary direction of flow, acetaminophen were formed upstream and sulfation occurred downstream, sequential processing would have occurred efficiently. In reality, the opposite is seen: enzymatic distributions are regionalized in a fashion which is the reverse of this optimized system. Hence, N flow directs formation of acetaminophen downstream and a reduced yield of the second product, acetaminophen sulfate conjugate; R flow, by virtue of reversal in recruitment of metabolic activities, results in acetaminophen formation upstream, a higher yield of the second product, and thus provides evidence of zonation (14).

When, in contrast, a substrate is converted to two products, upstream and downstream in relation to the ordinary direction of flow, R perfusion will enhance formation of the downstream product and reduce formation of the upstream product, in comparison with N flow (16, 17, 49). The N and R approach is therefore expected to become a routinely utilized tool in the assessment of product formation data in the intact liver; these explorations will be expected to provide insight into the relative acinar distributions of drug-metabolizing enzymes in this organ, during examinations of sequential and competitive drug and metabolite processing.

Acknowledgments: We thank Dr. Marilyn E. Morris, State University of New York at Buffalo, School of Pharmacy, and Wendy F. Cherry, Faculty of Pharmacy, University of Toronto, for assistance in the research. We are grateful to members of the Department of Pathology, Hospital for Sick Children, University of Toronto: Dr. M. J. Phillips, Head of Department, for his kind supervision of the microscopic work and use of the electron microscope facilities, Patricia Spicer and Vernon Edwards for providing instruction and assistance in electron microscope techniques, and to Mike Starr for help in the photography.

REFERENCES

1. Baron J, Redick JA, Guengerich FP. An immunohistochemical study on the localizations and distributions of phenobarbital and 3-methylcholanthrene inducible cytochromes P-450 within the livers of untreated rats. J Biol Chem 1981; 256:5931–5937.
2. Ullrich D, Fischer G, Katz N, et al. Intralobular distribution of UDP-glucuronosyltransferase in livers from untreated 3-methylcholanthrene and phenobarbital treated rats. Chem Biol Interact 1984; 48:181–190.
3. Moody DE, Taylor LA, Smuckler EA, et al. Immunohistochemical localization of cytochrome P-450a in liver sections from untreated rats and rats treated with phenobarbital or 3-methylcholanthrene. Drug Metab Dispos 1983; 11:339–343.
4. Moody DE, Taylor LA, Smuckler EA. Immunofluorescent determination of the lobular distribution of a constitutive form of hepatic microsomal cytochrome P-450. Hepatology 1985; 5:440–451.
5. Wattenberg LW, Leong JL. Histochemical demonstration of reduced pyridine nucleotide dependent polycyclic hydrocarbon metabolizing systems. J Histochem Cytochem 1962; 10:412–420.
6. Ji S, Lemasters JJ, Thurman RG. A fluorometric method to measure sublobular rates of mixed-function oxidation in the hemoglobin-free perfused rat liver. Mol Pharmacol 1981; 19:513–516.
7. Conway JG, Kauffman FC, Tsukada T, et al. Glucuronidation of 7-hydroxycoumarin in periportal and pericentral regions of the liver lobule. Mol Pharmacol 1984; 25:487–493.
8. Harris C, Thurman RG. A new method to study glutathione adduct formation in periportal and pericentral regions of the liver lobule by micro-reflectance spectrophotometry. Mol Pharmacol 1986; 29:88–96.
9. El Mouelhi M, Kauffman FC. Sublobular distribution of transferases and hydrolases associated with glucuronide, sulfate and glutathione conjugation in human liver. Hepatology 1986; 6:450–456.
10. deBaun JR, Smith JYR, Miller EC, et al. Reactivity in vivo of the carcinogen *N*-hydroxy-2-acetylaminofluorene: increase by sulfate ion. Science 1971; 167:184–186.
11. Meerman JHN, Mulder GJ. Prevention of the hepatotoxic action of *N*-hydroxy-2-acetylaminofluorene in the rat by inhibition of *N*-*O*-sulfation by pentachlorophenol. Life Sci 1981; 28:2361–2365.
12. Groothuis GMM, Meijer DKJ, Hardonk MJ. Morphological studies on selective acinar liver damage by *N*-hydroxy-2-acetylaminofluorene and carbon tetrachloride. Naunyn-Schmiedebergs Arch Pharmakol 1983; 322:298–309.
13. Trowell OA. Urea formation in the isolated perfused liver of the rat. J Physiol 1942; 100:432–458.
14. Pang KS, Terrell JA. Retrograde perfusion to probe the heterogeneous distribution of hepatic drug metabolizing enzymes in rats. J Pharmacol Exp Ther 1981; 216:339–346.
15. Pang KS, Stillwell RN. An understanding of the role of enzymic localization of the liver on metabolite kinetics: a computer simulation. J Pharmacokinet Biopharm 1983; 11:451–468.
16. Pang KS, Koster H, Halsema ICM, et al. Normal and retrograde perfusion to probe the zonal distribution of sulfation and glucuronidation activities of harmol in the perfused rat liver preparation. J Pharmacol Exp Ther 1983; 224:647–653.
17. Morris ME, Pang KS. Competition between two enzymes for substrate removal in liver: modulating effects of competitive pathways. J Pharmacokinet Biopharm 1987; 15:473–496.
18. Chen EH, Gumucio JJ, Ho NH, et al. Hepatocytes of zones 1 and 3 conjugate sulfobromophthalein with glutathione. Hepatology 1984; 4:467–476.
19. Pang KS, Terrell JA, Nelson SD, et al. An enzyme-distributed system for lidocaine metabolism in the perfused rat liver preparation. J Pharmacokinet Biopharm 1986; 14:107–130.
20. Groothuis GMM, Hardonk MJ, Keulemans KPT, et al. Autoradiographic and kinetic demonstration of acinar heterogeneity of taurocholate transport. Am J Physiol 1982; (Gastrointest Liver Physiol 6) 243:G455–G462.
21. Bass NM, Manning JA, Sorrentino D, et al. Increased organic anion extraction by retrograde perfused rat liver reflects increased sinusoidal volume (Abstract). Hepatology 1986; 6:354.
22. Otter WD, Tuit G. Causes of the zonal distribution of glycogen in the liver acinus after fat-rich diet. Anat Rec 1972; 173:325–332.
23. Häussinger D. Hepatocyte heterogeneity in glutamine and ammonia metabolism and the role of an intercellular glutamine cycle during ureagenesis in perfused rat liver. Eur J Biochem 1983; 133:269–275.
24. Scholmerich J, Kitamura S, Miyai K. Structural and functional integrity of rat liver perfused in backward and forward direction. Res Exp Med 1986; 186:397–405.

25. Goresky CA. A linear method for determining liver sinusoidal and extravascular volumes. Am J Physiol 1963; 204:626–640.
26. Goresky CA, Gordon ER, Bach GG. Uptake of monohydric alcohols by liver: demonstration of a shared enzymic space. Am J Physiol 1983; 244:G198–G214.
27. Isselbacher KJ, Carter, EA. Ethanol metabolism: oxidative and peroxidative mechanisms. Drug Metab Dispos 1973; 1:449–454.
28. Kashiwagi T, Ji S, Lemasters JJ, et al. Rates of alcohol dehydrogenase-dependent ethanol metabolism in periportal and pericentral regions of the perfused rat liver. Mol Pharmacol 1982; 21:438–443.
29. Pang KS, Schwab AJ, Goresky CA, et al. Effects of perfusate flow rate on measured blood volume, Disse space, intracellular water space, and drug extraction in the perfused rat liver preparation: characterization by the multiple indicator dilution technique. J Pharmacokinet Biopharm 1988; 16:595–632.
30. Meier P, Zierler KL. On the theory of the indicator-dilution method for measurement of blood flow and volume. J Appl Physiol 1954; 6:731–744.
31. Brien JF, Hoover DJ. Gas-liquid chromatographic determination of ethanol and acetaldehyde in tissues. J Pharmacol Methods 1980; 4:51–58.
32. Wisse E. Observations on the fine structure and peroxidase cytochemistry of normal rat liver Kupffer cells. J Ultrastruct Res 1974; 46:393–426.
33. Wisse E. An ultrastructural characterization of the endothelial cell in the rat liver sinusoid under normal and various experimental conditions, as a contribution to the distinction between endothelial and Kupffer cells. J Ultrastruct Res 1972; 38:528–562.
34. Kelman GR, Nunn JF. Computer produced physiological tables for calculations involving the relationships between blood oxygen tension and content. London: Butterworths, 1968.
35. Henry RJ, Cannon DC, Winkelman JW, eds. Clinical chemistry: principles and technics. Hagerstown, Maryland: Harper and Row, 1974: 1131–1135.
36. Brauer RW. Liver circulation and function. Physiol Rev 1963; 43:115–213.
37. Schimassek H. Perfusion of isolated rat liver with a semisynthetic medium and control of liver function. Life Sci 1962; 11:629–634.
38. Ross BD. Perfusion of individual organs. In: Perfusion techniques in biochemistry. Oxford: Clarendon Press, 1972: 175–179.
39. Keiding S, Vilstrup H, Hansen L. Importance of flow and hematocrit for metabolic function of perfused rat liver. Scand J Clin Lab Invest 1980; 40:355–359.
40. Steinberg D, Baldwin D, Ostrow B. A clinical method for the assay of serum glutamic-oxalacetic transaminase. J Lab Clin Med 1956; 48:144–151.
41. Květina J, Guaitani A. A versatile method for the *in vitro* perfusion of isolated organs of rats and mice with particular reference to liver. Pharmacology 1969; 2:65–81.
42. Bartošek I, Guaitani A, Garattini S. Long-term perfusion of isolated rat liver. Pharmacology 1972; 8:244–258.
43. Matsumara T, Thurman RG. Measuring rates of O_2 uptake in periportal and pericentral regions of liver lobule: stop-flow experiments with perfused liver. Am J Physiol 1983; 244:G656–G659.
44. Goresky CA, Cousineau D, Rose CP, et al. Lack of liver vascular response to carotid occlusion in mildly acidotic dogs. Am J Physiol 1986; 251 (Heart Circ Physiol 20):H991–H999.
45. Pang KS, Gillette JR. Kinetics of metabolite formation and elimination in the perfused rat liver preparation: differences between the elimination of preformed acetaminophen and acetaminophen formed from phenacetin. J Pharmacol Exp Ther 1978; 207:178–194.
46. Pang KS, Cherry WF, Accaputo J, et al. Combined hepatic arterial-portal venous and hepatic arterial-hepatic venous perfusions to probe the abundance of drug metabolizing activities: perihepatic venous O-deethylation activity for phenacetin and periportal sulfation activity for acetaminophen in the once-through rat liver preparation. J Pharmacol Exp Ther 1988; 247:690–700.
47. Matsumara T, Kashiwagi T, Meren H, et al. Gluconeogenesis predominates in periportal regions of the liver. Eur J Biochem 1984; 144:409–414.
48. Matsumara T, Thurman RG. Predominance of glycolysis in pericentral regions of the liver lobule. Eur J Biochem 1982; 140:229–234.
49. Morris ME, Yuen V, Tang BK, et al. Competing pathways in drug metabolism. I. Effect of varying input concentrations on gentisamide conjugation in the once-through *in situ* perfused rat liver preparation. J Pharmacol Exp Ther 1988; 245:614–624.